JPhys Energy

PAPER • OPEN ACCESS

Hydrogen production by the photoreforming of methanol and the photocatalytic water–gas shift reaction

Journal of Physics: Energy

OPEN ACCESS

RECEIVED
9 September 2020

REVISED
3 January 2021

ACCEPTED FOR PUBLICATION
19 January 2021

PUBLISHED
11 March 2021

PAPER

Hydrogen production by the photoreforming of methanol and the photocatalytic water–gas shift reaction

Julia Kennedy[1], James Hayward[1], Philip R Davies[1] and Michael Bowker[1,2]

[1] Cardiff Catalysis Institute, School of Chemistry, Cardiff University, Cardiff, CF10 3AD, United Kingdom
[2] UK Catalysis Hub, Research Complex at Harwell, Rutherford Appleton Laboratory, Harwell, OX11 0FA Oxon, United Kingdom

E-mail: bowkerm@cardiff.ac.uk

Keywords: photocatalysis, methanol, water splitting, titania, reforming, water gas shift

Abstract

We have examined the reforming of methanol and CO on Pd/P25 TiO_2 catalysts for hydrogen production, and compared it with rates for similarly supported Au and Cu catalysts. Both reactions proceed, but the photocatalytic water–gas shift (WGS) reaction is much slower than for methanol reforming. CO_2 is evolved as expected, but the yields can be much lower than for the expected stoichiometry ($CH_3OH + H_2O \rightarrow CO_2 + 3H_2$). We show that this is due to dissolution of the carbon dioxide into the aqueous phase. We have also carried out both reactions in the gas phase. Both proceed at a higher rate in the gas phase, and for methanol reforming, there is some CO evolution. In $H_2 + CO_2$ reactions, there is little sign of the reverse WGS reaction, but some photo-methanation does occur. Of the three catalysts Pd is the best for the methanol reforming reaction, while Au is best for the water–gas shift. Nonetheless, Cu works reasonably well for methanol reforming and makes a much cheaper, earth-abundant catalyst.

1. Introduction

The use of fossil fuels since the industrial revolution has increased the levels of CO_2 in the atmosphere from 280 ppm to over 400 ppm now [1]. CO_2 is a greenhouse gas and so with increasing CO_2 levels, the temperature of the Earth has increased, global warming. It is fossil fuels which mainly produce this extra CO_2, and so alternative, greener energy resources are being developed. The main one of these is hydrogen, produced using renewable energy via water splitting, usually by electrolysis [2]. The problem then is that hydrogen storage is expensive and as a gas it has low volume energy density. Hence there is a drive to store this energy in a denser liquid form, such as methanol, or maybe ammonia. Methanol is said to be 'the next chemical vector' after petrol as it is compatible with the existing petroleum infrastructure [3, 4].

Electrolysis is extremely expensive and generally does not benefit from scale cost reductions. Hence the interest in a more direct way of making hydrogen, and the direct use of photocatalytic water splitting is an interesting possibility. However, the thermodynamics indicate that this is extremely difficult (gas phase $\Delta H_0 = 242$ kJ mol^{-1}, $\Delta S_0 = 44$ J K^{-1} mol^{-1}; liquid phase $\Delta H_0 = 286$ kJ mol^{-1}, $\Delta S_0 = 163$ J K^{-1} mol^{-1}) [5], though some claim to be able to directly split water with complex catalysts, using visible light, though under vacuum conditions [6–8].

As a result, much of the work in this area involves the addition of sacrificial agents as hole scavengers, in order to make hydrogen production more feasible. Using methanol as a sacrificial agent for photocatalytic methanol reforming was first achieved in 1980 by Kawai and Sakata where hydrogen was produced using metal loaded titania [9]. This work was continued using IR spectroscopy to study the mechanism of photocatalytic methanol reforming by [10]. The proposed mechanism is shown below in reactions (1) and (2). It was concluded that the presence of CO_2 indicated that water was split

$$CH_3OH \rightarrow CH_3O_{(ads)} + H_{(ads)} \quad (1)$$

$$CH_3O_{(ads)} + H_2O \rightarrow CO_{2(g)} + 5/2\,H_{2(g)}\,. \quad (2)$$

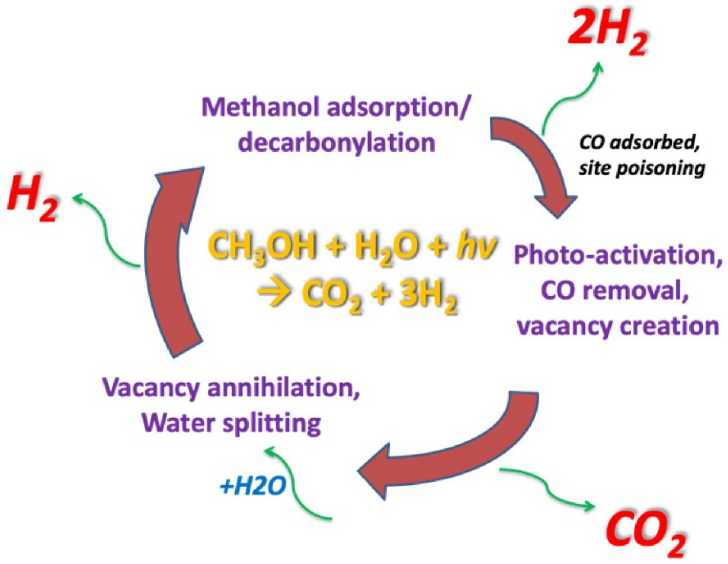

Figure 1. A schematic model of methanol photoreforming on metal/titania catalysts.

More recently, Bowker *et al* proposed a full mechanism for photocatalytic methanol reforming on Pd/TiO_2 [11–15], which is summarised in figure 1. A low rate dependence on methanol concentration was found, indicating a near zero-order dependence on methanol concentration which was attributed to saturation type kinetics (Langmuir Hinshelwood model). The mechanism involved decarbonylation of methanol on Pd to liberate hydrogen in a thermal reaction with the surface which leaves CO adsorbed on the metal, at which point reaction stops without light. Upon light exposure active oxygen (the hole, O^-, produced by electron–hole pair excitation) is produced on the support TiO_2 which removes CO from the metal and hence sustains steady-state CO_2 and H_2 production. In this condition, methanol is continuously adsorbing on the metal, decomposing to adsorbed CO and gas phase hydrogen, and the CO is being removed by the active oxygen (the holes) created on the titania by electron–hole pair excitation.

The oxidising species was suggested to be OH^-, OH• or O• [15]. In a recent study by Nomikos *et al* it was suggested that formic acid and formaldehyde stay adsorbed to the photocatalyst until full decomposition and oxidation to CO_2 [16].

Methanol is known to adsorb to metal oxides via the methoxy species [17]. Methanol readily produces formaldehyde under UV illumination [18, 19]. Decomposition to formaldehyde has been investigated by FTIR spectroscopy and the proposed mechanism is shown below in reactions (3)–(5) [20]

$$CH_3OH \rightarrow CH_3O^-{}_{(ads)} + H^+ \tag{3}$$

$$CH_3O^-{}_{(ads)} + H^+ \rightarrow CH_3O\bullet_{(ads)} \tag{4}$$

$$CH_3O\bullet_{(ads)} + h^+ \rightarrow CH_2O_{(ads)} + H^+. \tag{5}$$

It was suggested that the formaldehyde species does not desorb but undergoes further oxidation using surface oxygen ions ($O_{(s)}$) to form dioxymethylene, reaction (6)

$$CH_2O_{(ads)} + O_{(s)} \rightarrow H_2CO_{2(ads)}. \tag{6}$$

Dioxymethylene can then further consume photogenerated holes to produce formic acid and release photons. Finally the surface formic acid can be decarbonylated via the photo-Kolbe reaction [7, 21, 22], resulting in CO_2 and H_2 as shown in reaction (7)

$$H_2CO_{2(ads)} + h^+ \rightarrow HCOO_{(ads)} + H^+ \rightarrow CO_2 + H_2. \tag{7}$$

Intermediates have been reported for steam photoreforming of methanol and the photo-oxidation of methanol. Formaldehyde, formic acid and CO were detected for steam photoreforming [23]. Formaldehyde and formic were reported for photo-oxidation [24]. Phillips *et al* have shown that methyl formate can be

produced by photo-oxidation and that the holes are pivotal to the reaction [25]. In both that paper and that of Setvin *et al* methyl formate can be produced by reaction of formaldehyde and methoxy units under illumination and holes or surface hydroxyl groups determine the reaction pathways [26]. It is certainly the case however, that if species such as formic acid or formaldehyde are present in solution, they must be there at a low level, since the former decomposes to CO_2 and H_2 without light and the latter is converted photocatalytically at a similar rate to methanol [11].

It must be noted that many other oxygen containing compounds have been used for photocatalytic hydrogen production including ethanol [27], n-butanol [28], glycerol [29, 30], and sugars such as glucose, and rules which dictate their efficacy have been defined [31].

There is another important reaction related to methanol reforming (equation (8)) and that's the so-called water–gas shift (WGS) reaction (equation (9))

$$CH_3OH + H_2O \rightarrow CO_2 + 3H_2, (\Delta H_r{}^0 = 50\,kJ\,mol^{-1}; \Delta S_r{}^0 = 175\,JK^{-1}\,mol^{-1})^5 \quad (8)$$

$$CO + H_2O \rightarrow CO_2{+}H_2, (\Delta H_r{}^0 = -39\,kJ\,mol^{-1}; \Delta S_r{}^0 = -42\,JK^{-1}\,mol^{-1})^5. \quad (9)$$

This reaction is also considered here, since both reactants are produced during the reaction and the formation of products in this way is not so often reported. So, the aims of this paper are to report investigations into the photocatalytic WGS reaction and to what extent it can be used to produce H_2, together with considerations of what role, if any, the WGS might play in methanol photoreforming.

2. Experimental

2.1. Catalyst preparation

Metal deposition was carried out using the incipient wetness technique. $PdCl_2$ (Sigma Aldrich) was dissolved in the appropriate amount of deionised water and two drops of HCl added. The solution was added slowly to P25 TiO_2 with stirring. The catalyst was then dried at 120 °C for 2 h, then calcined at 400 °C for 3 h and was finally ground and passed through a 53 μm sieve to ensure a small particle size. The P25 is a mix of ∼20% rutile, with the majority being anatase, and the Pd nanoparticles are too small to be seen in our electron microscope (and that is also reported by others [32, 33]) and XRD at this loading. However at 0.6% loading using sol immobilisation methods, the particles have an average size of around 3 nm [34], whereas using incipient wetness, as here, 3% loading gave a particle size of ∼2.5 nm [33].

2.2. Photoreactor

This comprised a photoreactor, light source and analysis was by gas chromatography (GC). The photoreactor involved using a Pyrex two necked flask, one for purging with nitrogen and the other for sampling. The size of vessel was 200 ml in total and the thickness of the glass was 2 mm (minimising light absorption). The vessel was clamped above a hot plate so that the reaction could be stirred and heated if necessary. The light source was placed 30 cm away from the front of the vessel. The reactor and lamp were placed inside a black Perspex box to minimise interference from other light sources and light emission into the laboratory. Samples were taken at regular intervals from the reactor before, during and after the experiment and analysed using a GC.

In the reaction vessel, the catalyst (0.2 g) and deionised water (usually 100 ml) were purged with nitrogen for 30 min to remove oxygen and other gases. The alcohol (0.00247 mol) was added to the reaction mixture via syringing through a rubber bung. The mixture was stirred using a magnetic stir bar. The lamp was then turned on illuminating the front of the flask. 0.2 ml samples were taken every 30 min and analysed using a GC to detect hydrogen. Some reactions required another GC to detect CO_2, CO and CH_4. For gas phase reactions the catalyst (0.2 g) was fixed on to a glass slide and secured above the water (usually 10 ml) and alcohol (usually 0.0024 mol) mixture.

A xenon arc lamp (Oriel Model No: 6271) was used to replicate sunlight in the photocatalytic experiments. The lamp along with the ignitor, condensing optics, rear reflector and lamp cooling fan were placed in an arc lamp housing (Oriel Model No: 66 921). This was then connected to a power supply (Newport Model No: 69 920).

GC was used to identify and quantify the products from photocatalytic reactions. Samples were taken before, during and after reaction using a gas syringe. Two GCs were used during this study to analyse hydrogen production. The first was a Varian 3300 using a 2 m long, molecular sieve, 13X column and a TCD. When this GC became inoperable analysis was continued using a Perkin Elmer Clarus 480 equipped with a 2 m × 1/8 in, silicostel molecular sieve and TCD. 0.2 ml was extracted from the reaction system using a gas tight syringe (from SGE) and injected into the GC. The column used was capable of separating hydrogen,

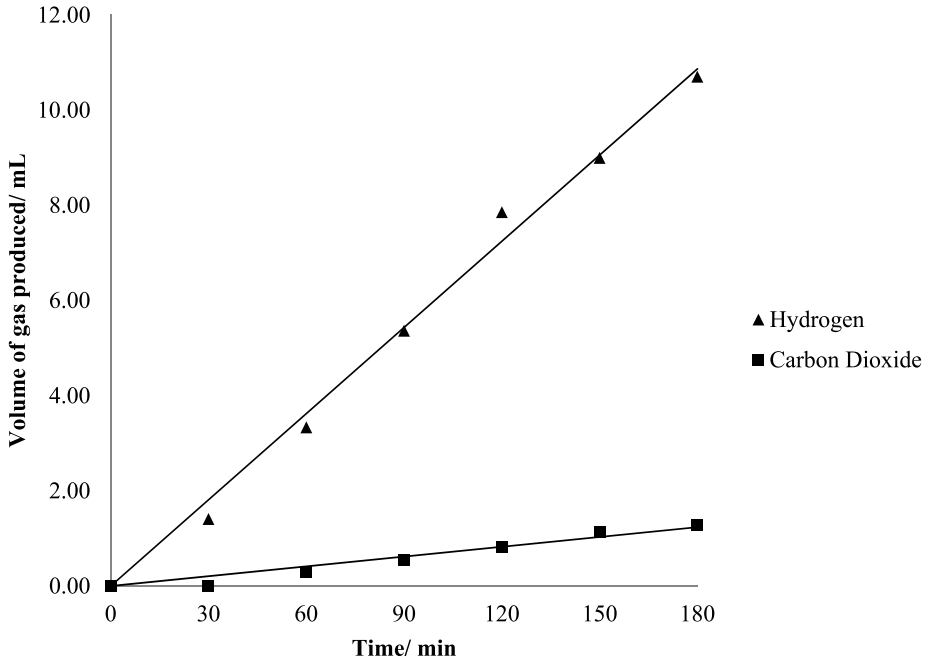

Figure 2. H_2 and CO_2 production over time for photocatalytic methanol reforming using 0.5% Pd/TiO_2 in the liquid phase (100 ml water). The lines are simple linear fits to the data.

oxygen, nitrogen and CO. Due to the difference in thermal conductivity between argon and hydrogen, argon was used as the carrier gas.

To measure other gaseous products and liquid products a Perkin Elmer Clarus 480 was used. This system was equipped with two detectors; a thermal conductivity detector (TCD) and flame ionisation detector (FID). The method for analysing other gas samples was the same as for hydrogen but using a different column and carrier gas. The column used was a 5 ft × 1/8 in × 2.1 mm SS (Suplico Analytical) and the carrier gas was helium.

Some of the experiments were carried out in a different reactor (figure 8). Catalysts were tested for photocatalytic water–gas shift activity in a windowed autoclave with an internal volume of 16 cm^3. Twenty milligrams of catalyst was dispersed in deionised water via sonication for 30 min, with the dispersion then being transferred to a quartz disc and dried for 1 h at 110 °C. The system was purged with flowing nitrogen (20 ml min^{-1}, 30 min) and then the reactants were supplied by flowing CO through a water bubbler (20 ml min^{-1}, 30 min). The system was then sealed and illuminated using a Quantum Devices Xe Arc Lamp solar simulator with a power of approximately 100 mW cm^{-2} for 2 h. The products were collected and analysed offline by a Bruker RGA GC with channels for hydrogen detection, permanent gas detection, and hydrocarbon detection.

3. Results and discussion

3.1. Methanol photoreforming

The proposed overall reaction scheme for methanol reforming is shown in reaction (8) and figure 1 above [11–14]. The stoichiometric relationship between hydrogen and carbon dioxide is 3 moles H_2 to 1 mole of CO_2.

The yield of hydrogen and carbon dioxide was monitored over time to establish whether the reaction followed this stoichiometry, see figure 2. Both H_2 and CO_2 are produced at a steady rate, though there may be some short induction time before CO_2 is seen. The presence of CO_2 suggests that water has been split according to the reaction and is further evidence of the mechanism proposed by Bowker *et al* [11–14]. After 3 h of reaction, 10.7 ml of H_2 has been evolved but only 1.3 ml of CO_2. The H_2:CO_2 ratio here is much higher than the expected 3:1. High H_2:CO_2 ratios have been reported in the literature and it was suggested that it was due to incomplete oxidation of CO_2 with CO being detected [35]. During this experiment, however, no CO was detected suggesting that either CO is still adsorbed on the palladium surface or complete oxidation occurred only producing CO_2. We suggest that the cause of the high H_2:CO_2 ratio is the well-known high solubility of CO_2 in water solution, and this is considered further below.

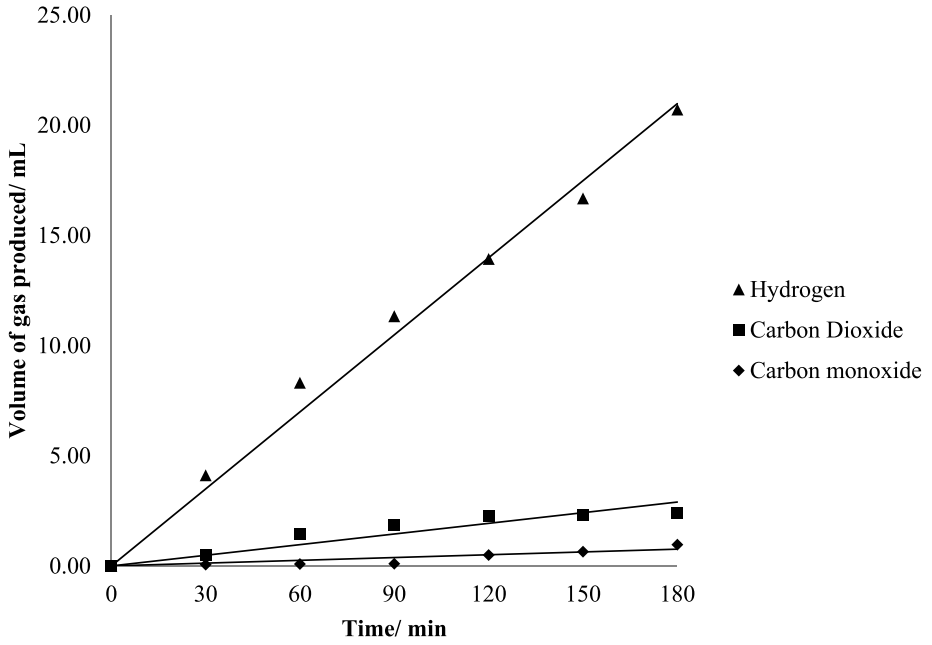

Figure 3. H_2 and CO_2 production over time for photocatalytic methanol reforming using 0.5% Pd/TiO_2 in the gas phase (10 ml water). The lines are simple linear fits to the data.

The experiment was repeated in the gas phase to probe whether this would have an effect on the H_2:CO_2 ratio. Figure 3 shows hydrogen, carbon dioxide and carbon monoxide production over time using 10 ml water. Now a small amount of CO was also observed during the reaction.

There is a higher rate of hydrogen production in the gas phase compared to the liquid phase with 21 ml of hydrogen produced in the gas phase but only 11 ml in the liquid phase within 3 h. It is possible that there is a higher ratio of methanol to water in gas phase reactions. Raoult's law allows us to calculate the approximate vapour pressure of water and methanol at a particular temperature. The temperature of the reaction here is 40 °C. At this temperature the vapour pressure of pure methanol is 229 mm Hg [36] and the vapour pressure of pure water is 55 mm Hg [35]. Using Raoult's Law the vapour pressure during the gas phase reaction was calculated to be 1 mm Hg for methanol and 55 mm Hg for water. This gives a ratio of methanol to water of 1:55. In the liquid phase the molar ratio of methanol to water is 1:2230. This suggests that in the gas phase there would be less competition between methanol and water for the active sites on Pd, leading to a higher rate of methanol decomposition and therefore a higher rate of hydrogen production.

The presence of CO in the gas phase reaction and not in the liquid phase reaction is interesting. We have previously proposed that adsorbed CO is an intermediate during photocatalytic methanol reforming [11–14], see figure 1. It is possible that desorption of CO happens more readily in the gas phase compared to the liquid phase. This could be due to the higher temperature of the gas phase reaction (55 °C vs 40 °C for the catalyst in the liquid phase). It has been reported that CO can start to desorb from Pd even at 300 K, at least when the coverage is very high, with more desorbing with increasing temperature [37]. In a continuous flow study of methanol/water reforming in the gas phase Caravaca *et al* [38] showed that thermal methanol dehydrogenation to CO dominated over photoreforming at elevated temperatures, but photoreforming dominated at 100 °C. At that temperature the CO production was significant and greater than CO_2. Another possibility is that the CO_2 produced during the reaction is reacting with the vacancies in the TiO_2 lattice more efficiently in the gas phase than in the liquid phase. Finally, as reported below, the WGS reaction occurs in this system, and this may be more efficient in the aqueous phase when CO is produced in that phase.

Let us now turn to how this reaction proceeds. The mechanism we propose for the reaction can be summarised as follows, and as shown in figure 4, which is a more detailed picture than figure 1. The first reactive step involves methanol dehydrogenation

$$CH_3OH \rightarrow CO_a + 2H_2$$

where CO_a refers to carbon monoxide adsorbed on the Pd nanoparticles, and as shown in figure 4(a). That this occurs at ambient temperature on pure Pd, as has been shown previously [39, 40]. At this point the

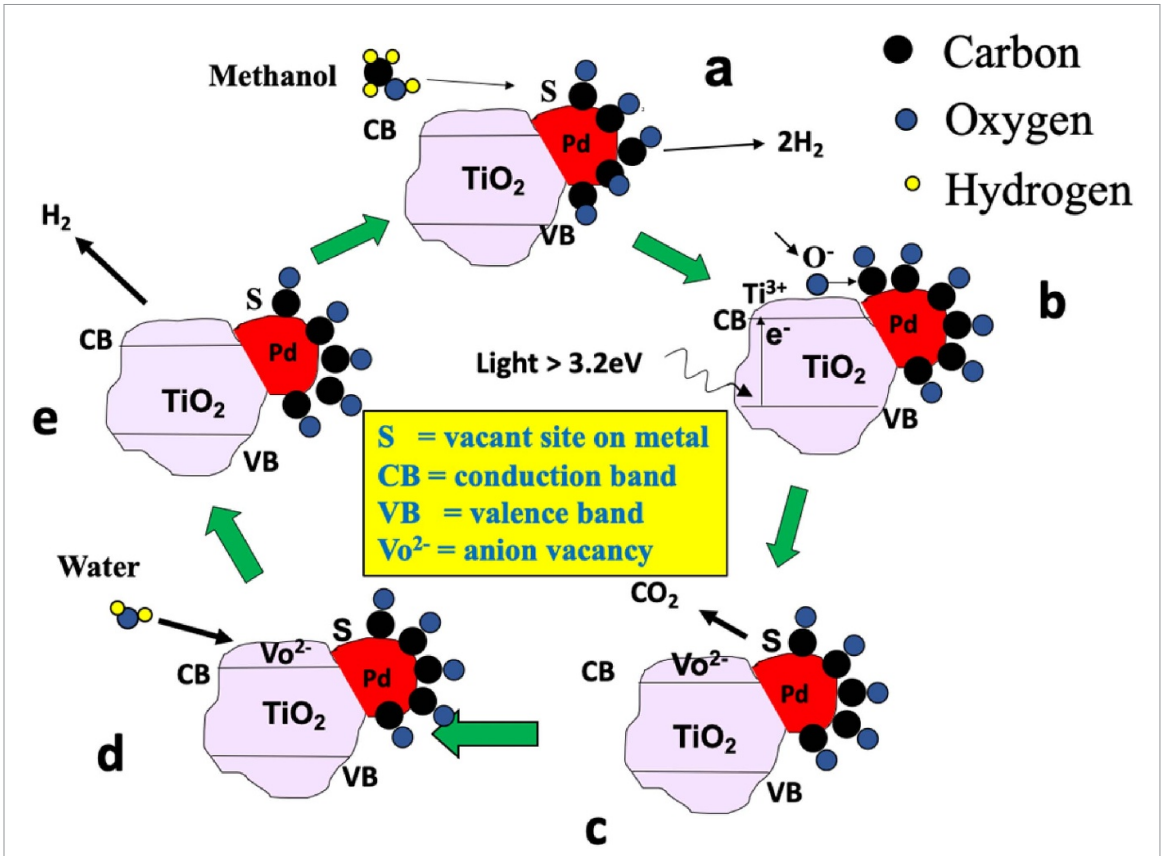

Figure 4. Schematic diagram of the photocatalytic reforming of methanol on the Pd/TiO_2 catalysts.

surface becomes unreactive, due to adsorbed CO blocking further methanol adsorption [40], and reaction only resumes when light is introduced to the system (figure 4(b)). At that point CO_2 and H_2 begin to evolve from the reaction at steady state because electron–hole pair separation occurs by bandgap excitation, and the hole (effectively O^-) is a highly reactive oxidant, attacks the CO at the periphery of the nanoparticles, producing CO_2 as follows

$$Ti^{4+}O^{2-} + h\nu \rightarrow Ti^{3+}O^{-}$$

$$CO_a + Ti^{3+}O^{-} \rightarrow CO_2 + S + Ti^{3+}V_o{}^{-}.$$

This then leaves a vacancy for further methanol adsorption and decomposition on the metal (S, figure 4(c)). However, the loss of oxygen from the titania leaves an anion vacancy (figure 4(c)) and for steady-state reaction this must be re-oxidised and the only oxidant available is water, figure 4(d), and this completes the photocatalytic cycle.

$$Ti^{3+}V_o{}^{-} + H_2O \rightarrow Ti^{4+}O^{2-} + H_2.$$

In order to further investigate the proposal that CO_2 solubility is the cause of the low amount of CO_2 detected, the gas phase reaction was also carried out with lower amounts of water in the reservoir below the sample. As figure 3 shows, using 10 ml water 21 ml of H_2, 2.4 ml CO_2 and 0.96 ml CO were produced in 3 h. This is a H_2:CO_2 ratio of 8.7:1. Incorporating CO into the ratio (H_2:C) calculation gives 5.6:1 which is closer to the expected 3:1 ratio. The volume of water used during photocatalytic methanol reforming was reduced to 1 ml which gave a H_2:CO_2 ratio of 5.4:1 and H_2:C ratio of 3.8:1 (figure 5). Therefore, this suggests that with less water present in the reservoir to absorb the CO_2, a better stoichiometric relationship in the gas phase products is achieved.

The pH of the water was recorded before and after reaction and it was noted that the pH decreased. CO_2 dissolves in water reacts with water to produce carbonic acid (reaction (10)).

$$CO_2 + H_2O \rightleftharpoons H_2CO_3. \quad (10)$$

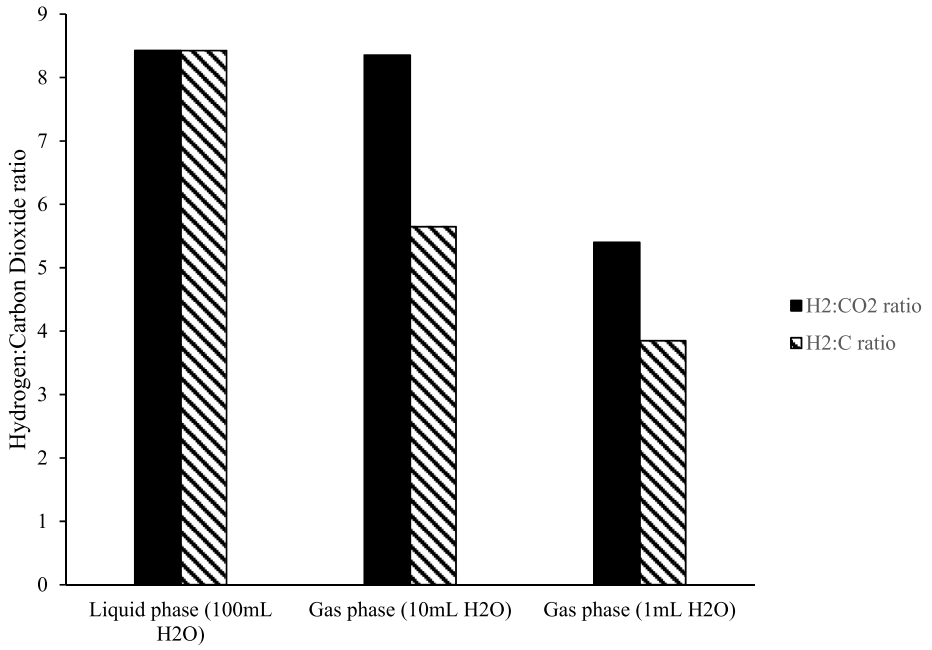

Figure 5. Ratio of H_2:CO_2 and H_2:C for photocatalytic methanol reforming in liquid phase and gas phase.

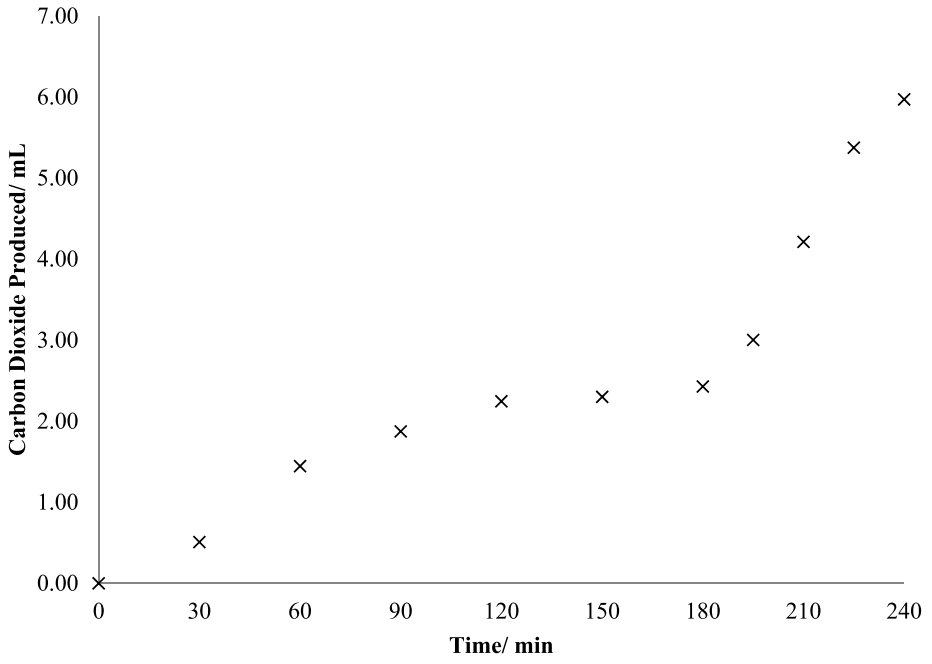

Figure 6. CO_2 level throughout photocatalytic methanol reforming and after reaction, during heating to 60 °C. The lamp was switched off at 180 min when the heating began.

The observed decrease in pH confirms that some of the CO_2 produced during the reaction is dissolved in the reaction solution. To further confirm whether this was happening the reaction solution (gas phase, 10 ml water) was heated after the reaction and the level of CO_2 was measured (figure 6).

This shows that heating the reaction solution after the reaction evolves CO_2. This is evidence that the CO_2 produced during the reaction was dissolving in the reaction solution. After heating at 60 °C for 1 h, the level of CO_2 had risen to 6 ml. Thus the ratio of H_2:CO_2 after heating was found to be 3.5:1, and 3:1 if the CO is included. Therefore this has demonstrated that hydrogen and carbon dioxide are produced in a ∼3:1 ratio which is provides further support for the proposed mechanism (reaction (8)).

We also compared these data with those for Au and Cu at the same loading as Pd, and it can be seen that the performance is similar for Au and Cu, but with roughly half the yield as for Pd, table 1.

Table 1. Rates of hydrogen evolution from liquid phase methanol reforming on 0.5 wt% loading of three metals.

Metal	Rate of H2 production (ml h^{-1})
Pd	3.7
Au	1.7
Cu	1.6

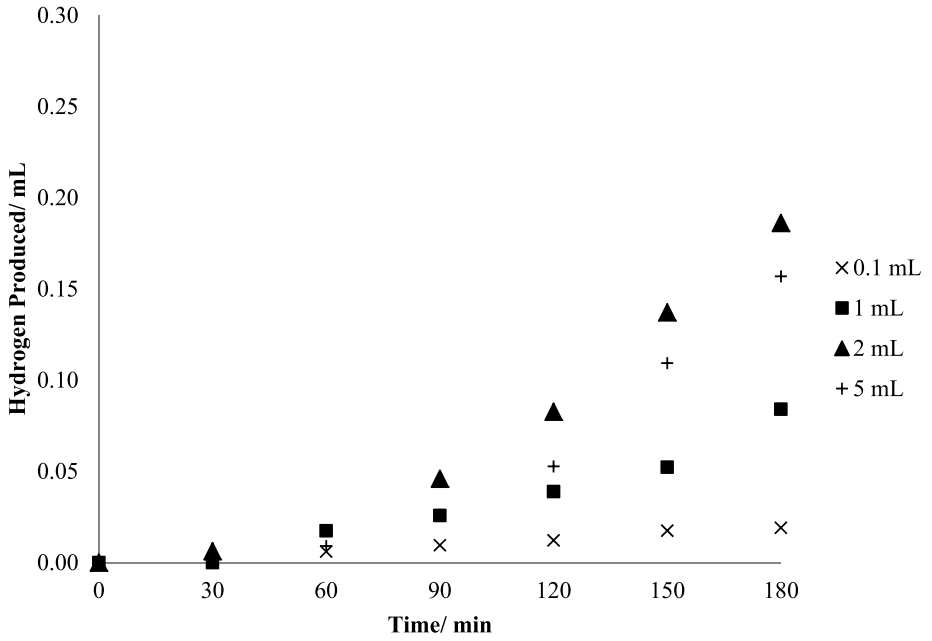

Figure 7. Hydrogen production using CO and 0.5% Pd/TiO_2 in water.

3.2. The photocatalytic water–gas shift reaction

It has been reported that methanol decomposes on Pd to form adsorbed CO at ambient temperatures [41]. The proposed mechanism for photocatalytic methanol reforming suggests that it is adsorbed CO that is oxidised by the active oxygen species (O^-) made by electron–hole excitation to produce an anion vacancy in TiO_2, allowing water to be split, as shown in figure 1. Therefore, it should be possible to use CO as the sacrificial agent/hole scavenger via the WGS reaction, and so here we report the results for the reaction, but carried out at ambient temperature, much lower than for the thermal reaction [42].

The volume of gas phase CO added to the flask was varied and the rate of hydrogen production was recorded (figure 7). This shows that hydrogen production increases with the amount of CO until 2 ml of gas have been added to the flask. Using 5 ml CO gives a slight reduction in hydrogen production. The trend is similar to work by Bowker *et al* where a maximum CO volume was observed [42]. After 1 ml the hydrogen yield dropped, with 10 ml CO producing almost no hydrogen. This suggests that the catalyst has become near-saturated and the availability of free sites for adsorption is low.

The reaction using CO as a sacrificial agent was carried out in both the gas and liquid phases to establish whether the same trend is seen as for methanol, where higher hydrogen yields were found for the gas phase reaction. The hydrogen produced from CO (2 ml) is shown below for the liquid phase and gas phase reactions (figure 8).

Figure 8 shows that 2 ml CO in the gas phase generates, like methanol, approximately double that which is produced in the liquid phase. The solubility of CO in water is 27.6 mg l^{-1}. This means that the majority of the CO will be in the gas phase, in this case where 10 ml of water is used. Therefore in the gas phase there is likely to be a higher $CO:H_2O$ ratio, meaning less competition with water, generating more hydrogen, but as mentioned above the sample temperature is also a little higher in the gas phase.

The liquid phase reaction with CO was repeated, however this time the reaction solution was left for 1 h prior to turning on the lamp to allow the CO more time to dissolve into the water. Figure 8 shows that there is not a significant difference between the two.

The reactions using CO are further proof of the proposed mechanism and also highlight the effect of competition with water on the hydrogen yield. The yield of hydrogen is very low compared with that from methanol, but this is probably due to a combination of reasons. Firstly, even if all other factors were the same,

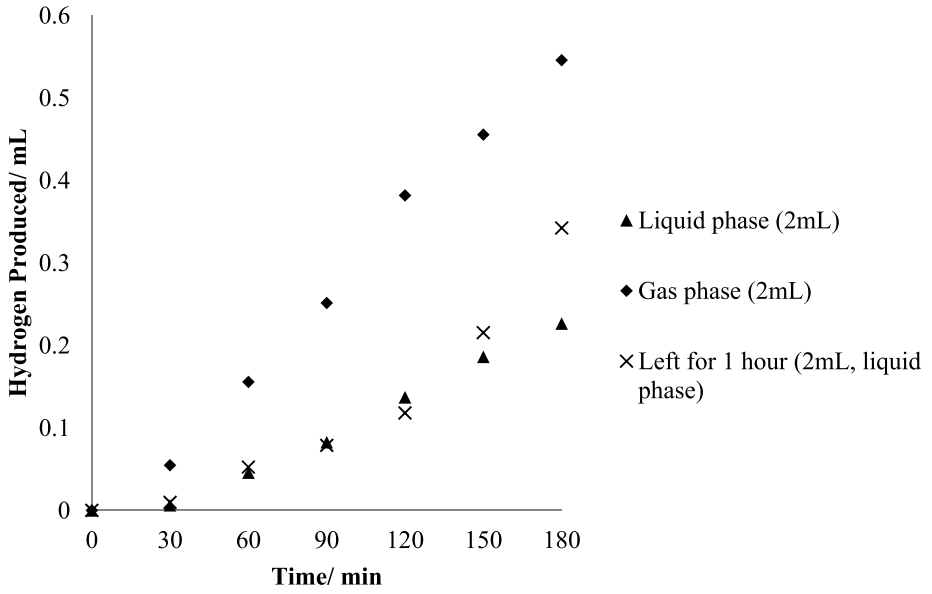

Figure 8. Hydrogen production using CO and 0.5% Pd/TiO_2 in liquid and gas phase.

Table 2. Gas production in micromole g^{-1} from the catalysts in figure 8.

Catalyst	H_2	CO_2	CH_4
TiO_2	0	0	0
Pd/TiO_2	464	530	24
Au/TiO_2	1215	1555	36
Cu/TiO_2	66	95	11

the stoichiometry of the reaction would produce 1/3rd the amount of hydrogen (reactions (8) and (9)). However, comparing the hydrogen production in figures 2 and 6, the hydrogen from CO is still low by a factor of 12 or so, even after taking the stoichiometry into account. Of course, a major difference between the two reactions is that the concentration of methanol in solution is around 25 times more than that of CO. The further contrast, however, is that in this range of concentration variation the rate from methanol becomes near zero order [13], whereas for CO above it becomes negative [42].

Thus, it is clear that the WGS reaction can take place photocatalytically at near room temperature. This further implies that CO can be converted to CO_2, and perhaps explains why none is seen in the liquid phase reaction of methanol (figure 2); but why is it seen in the gas phase reactions (figure 3)? This may be because the gas has to first proceed through the liquid phase in the former, with a high probability of further encounter with the dispersed catalyst particles, whereas once produced in the gas phase reaction it can escape from the fixed catalyst and only reacts slowly once in that phase.

In a different photoreactor (see appendix) broadly similar results were obtained for the WGS reaction, as shown in figure 9 below. In this case data for three different metals are shown, and it is clear that, although Au photocatalysts of this type are not as good as Pd for methanol photoreforming [43], they are considerably better for the photocatalytic WGS. Interestingly, there is also a small amount of methane produced on the three metals (figure 9 and table 2). The reaction between CO_2 and H_2 was measured to check for any occurrence of the reverse WGS reaction, carried out at low temperature, but no CO was produced, though some methane was produced from Pd. Note that although Cu was less active, it is a much more earth-abundant material and costs approximately 1/3000th the price of Au/mol, and it has similar activity to gold for methanol reforming, both of which have around half the rate for Pd.

In conclusion we have shown that Pd photocatalysts subtend the photoreforming of methanol to produce hydrogen and carbon dioxide. The latter may be observed to evolve in smaller than expected amount, due to the high solubility in water. Higher rates of hydrogen production (by a factor of ~2) are gained when the experiment is carried out in the gas phase, and then small amounts of CO are also produced. CO can also be reformed photocatalytically to produce hydrogen (photocatalytic WGS reaction), but at a much lower rate than for methanol. Au appears to be a much better catalyst for that reaction, giving three fold higher rates than Pd. These findings support a model in which methanol is initially decomposed on the metal

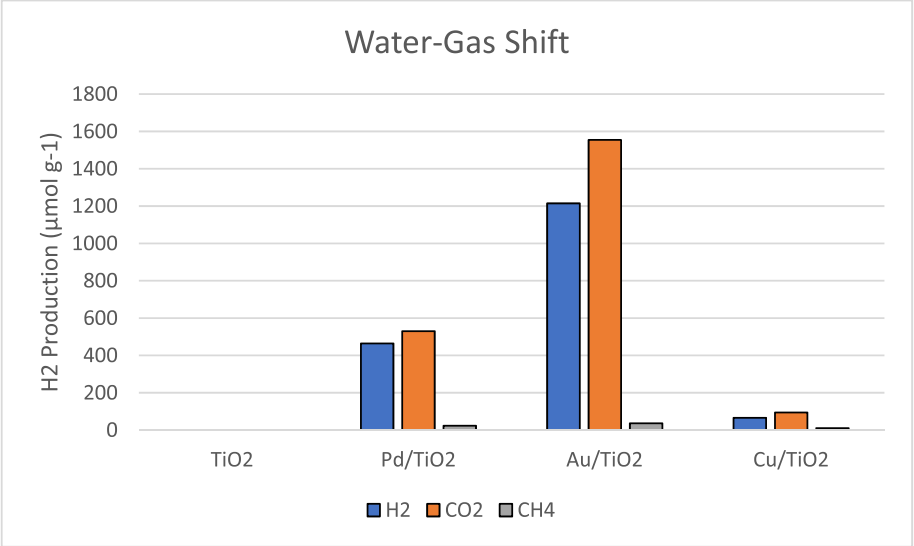

Figure 9. The photocatalytic water–gas shift reaction on P25 titania and loaded with 5 wt% of three metals by sol immobilisation, followed by calcination and reduction at 400 °C. Amount of hydrogen after 2 h of reaction.

nanoparticles,leaving CO strongly adsorbed there, and which therefore acts as a poison to the steady-state catalytic reaction. However, when exposed to UV light, reactive oxygen species (O^-, the hole) are produced on the TiO_2 by electron–hole excitation, which can then remove the CO as CO_2, and give anion vacancy sites in the lattice which are capable of reducing water, and so maintain a steady-state reaction.

Acknowledgments

We are grateful to Diamond Light Source for a part studentship to PH and for support from the UK Catalysis Hub, funded through EPSRC Grants EP/R026939/1 and EP/R026815/1, and from EPSRC EP/S030468/1, EP/N010531/1.

ORCID iD

Michael Bowker https://orcid.org/0000-0001-5075-1089

References

[1] Tans P 2021 *NOAA/ESRL* (available at: www.esrl.noaa.gov/gmd/ccgg/trends/)
[2] Shiva Kumar S and Himabindu V 2019 *Mater. Sci. Energy Technol.* **2** 442
[3] Grochala W and Edwards P P 2004 *Chem. Rev.* **104** 1283
[4] Olah G A, Goeppert A and Surya Prakash G K 2006 *Beyond Oil and Gas: The Methanol Economy* (New York, NY: Wiley)
[5] NIST, USA 2015 Numbers derived from heats of formation *Handbook of Chemistry and Physics* 96th edn, ed W M Haynes (London: CRC Press)
[6] Wang Q *et al* 2019 *Nat. Mater.* **18** 827
[7] Wang Q, Hisatomi T, Katayama M, Takata T, Minegishi T, Kudo A, Yamada T and Domen K 2017 *Faraday Discuss.* **197** 491
[8] Pan C, Takata T, Nakabayashi M, Matsumoto T, Shibata N, Ikuhara Y and Domen K 2015 *Angew. Chem., Int. Ed.* **54** 2955
[9] Kawai T and Sakata T 1980 *J. Chem. Soc. Chem. Commun.* **15** 694
[10] Kawai M, Naito S, Tamaru K and Kawai T 1983 *Chem. Phys. Lett.* **98** 377
[11] Dickinson A, James D, Perkins N, Cassidy T and Bowker M 1999 *J. Mol. Catal.* A **146** 211
[12] Bowker M, James D, Stone P, Bennett R A, Perkins N, Millard L, Greaves J and Dickinson A 2003 *J. Catal.* **217** 427
[13] Bowker M 2011 *Green Chem.* **13** 2235
[14] Bingham M, O'Rourke C and Bowker M 2019 *J. Photochem. Photobiol.* **373** 122
[15] Bowker M, Millard L, Greaves J, James D and Soares J 2004 *Gold Bull.* **37** 170
[16] Nomikos G N, Panagiotopoulou P, Kondarides D I and Verykios X E 2014 *Appl. Catal.* B **146** 249
[17] Akarmazyan S S, Panagiotopoulou P, Kambolis A, Papadopoulou C and Kondarides D I 2014 *Appl. Catal.* B **145** 136
[18] Chojnowski F, Clechet P, Martin J R, Herrmann J M and Pichat P 1981 *Chem. Phys. Lett.* **84** 555
[19] Pichat P, Mozzanega M N, Disdier J and Herrmann J M 1982 *Nouv. J. Chim. New J. Chem.* **6** 559
[20] Chen T, Feng Z, Wu G, Shi J, Ma G, Ying P and Li C 2007 *J. Phys. Chem.* C **111** 8005
[21] Zheng X, Wei L, Zhang Z, Jiang Q, Wei Y, Xie B and Wei M 2009 *Int. J. Hydrog. Energy* **34** 9033
[22] Nosaka Y, Koenuma K, Ushida K and Kira A 1996 *Langmuir* **12** 736
[23] Chiarello G L, Forni L and Selli E 2009 *Catal. Today* **144** 69
[24] Kandiel T A, Dillert R, Robben L and Bahnemann D W 2011 *Catal. Today* **161** 196

[25] Phillips K R, Jensen S C, Baron M, Li S-C and Friend C M 2013 *J. Am. Chem. Soc.* **135** 574
[26] Setvin A, Shi X, Hulva J, Simschitz T, Parkinson G S, Schmid M, di Valentin C, Selloni A and Diebold U 2017 *ACS Catal.* **7** 7081
[27] Yang Y Z, Chang C H and Idriss H 2006 *Appl. Catal.* B **67** 217
[28] Bahruji H, Bowker M, Davies P R and Pedrono F 2011 *Appl. Catal.* B **107** 205
[29] Bowker M, Davies P R and Al-Mazroai L S 2009 *Catal. Lett.* **128** 253
[30] Fu X, Wang X, Leung D Y C, Gu Q, Chen S and Huang H 2011 *Appl. Catal.* B **106** 681
[31] Fu X, Long J, Wang X, Leung D Y C, Ding Z, Wu L, Zhang Z, Li Z and Fu X 2008 *Int. J. Hydrog. Energy* **33** 6484
[32] Al-Azri Z H N, Chen W T, Chan A, Jovic V, Ina T, Idriss H and Waterhouse G I N 2015 *J. Catal.* **329** 355
[33] Bowker M, Maschmeyer T, Hartley G, Masters A, Jones W and Martin D J 2019 *Appl. Catal.* B **240** 373–9
[34] Naldoni A, D'Arienzo M, Altomare M, Marelli M, Scotti R, Morazzoni F, Selli E and dal Santo V 2013 *Appl. Catal.* B **130** 239
[35] Lide D R 1974 *CRC Handbook of Chemistry and Physics* 55th edn (Cleaveland, OH: CRC Press)
[36] Dean J A 1999 *Lange's Handbook of Chemistry* 15th edn (New York, NY: McGraw-Hill)
[37] Kaden W E, Kunkel W A, Roberts F S, Kane M and Anderson S L 2012 *J. Chem. Phys.* **136** 204705
[38] Caravaca A, Daly H, Smith M, Chansaiac M A and Hardacre C 2016 *React. Chem. Eng.* **1** 649
[39] Davis J L and Barteau M A 1987 *Surface Sci.* **187** 387
[40] Francis S, Corneille J, Goodman D W and Bowker M 2016 *Surface Sci.* **364** 30
[41] Christmann K and Demuth J E 1982 *J. Chem. Phys.* **76** 6318
[42] Millard L and Bowker M 2002 *J. Photochem. Photobiol.* A **148** 91
[43] Greaves J, Al-Mazroai L, Nuhu A, Davies P R and Bowker M 2006 *Gold Bull.* **39** 219